Brodogradnja Volume 77 Number 3 (2026) 77310

University of Zagreb
Faculty of Mechanical
Engineering and Naval
Architecture

journal homepage: www.brodogradnja.fsb.hr

Brodogradnja

An International Journal of Naval Architecture and
Ocean Engineering for Research and Development

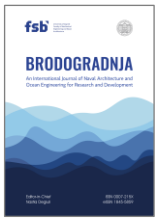

Battery remaining useful life estimation process design in hybrid ships: a case of data-driven algorithms

Tayfun Uyanık[*]

İstanbul Technical University, Maritime Faculty, 34940, Tuzla, İstanbul, Türkiye

ARTICLE INFO

Keywords:
Hybrid ships
Batteries
Energy efficiency
Data-driven algorithms
Remaining life prediction

ABSTRACT

Hybrid propulsion systems increase ship energy efficiency by allowing the sharing of power between diesel engines and battery energy storage systems. However, the long-term efficiency of these types of systems depends on accurately estimating the Remaining Useful Life (RUL) of lithium-ion batteries to allow effective charge scheduling, maintenance planning, and reliable navigation. This study uses nine data-driven algorithms, including ensemble methods, recurrent neural networks, and linear models, to examine the RUL of a lithium-ion battery pack installed on a hybrid cargo ship. A 5-fold cross-validation structure was used to preprocess, normalize, and analyze actual operational data gathered during the vessel's service life. To improve the accuracy of predictions, hyperparameter optimization was performed out. Long Short-Term Memory (LSTM), which reduced MAE from 2.87 to 1.46 and RMSE from 12.57 to 6.34 after optimization while retaining a high coefficient of determination ($R^2 = 0.9999$), performed the best among the models that were evaluated. The results obtained indicate that condition-based maintenance and energy utilization methods on hybrid ships can be effectively supported by data-driven RUL estimation. In order to enhance generalization and assess integration with real-time propulsion control systems, future research will expand the analysis to multi-vessel datasets.

1. Introduction

The maritime transportation sector is pivotal in the global economy, facilitating over 90 % of worldwide trade [1]. However, in recent years, emissions and global warming have increased dramatically due to ships' reliance on traditional power systems [2]. The objective of the Paris Agreement is to keep the rise in the global temperature to 1.5°C below pre-industrial levels, which underlines the necessity to reduce emissions of greenhouse gas (GHG) [3]. The International Maritime Organization (IMO) proposed activities to reduce pollution in the marine industry and try to address this issue. Several approaches that have been set in the scientific literature for promoting energy efficiency and reducing GHG emissions in the maritime sector have come forward in response to achieving the reduction goals set by the IMO and the Paris Agreement. These methods contain battery-powered propulsion, advanced combustion systems, cold-ironing, waste heat recovery, renewable energy sources, and hybrid propulsion. Among these methods, hybridizing vessels by integrating internal combustion engines and electric motors is a promising solution [4]. However, the

[*] Corresponding author.
E-mail address: uyanikt@itu.edu.tr

https://doi.org/10.21278/brod77310
Received 20 October 2025; Received in revised form 28 November 2025; Accepted 8 January 2026
Available online 19 January 2026
ISSN 0007-215X; eISSN 1845-5859

successful adoption of this transformative approach necessitates the development of an intelligent energy management system capable of optimizing performance while minimizing emissions, thereby advancing sustainability goals in maritime transportation.

The electrification of ships is a substantial and dynamic research domain incorporating multiple focus areas. Researchers explore power systems [5], energy management [6], electric propulsion [7], power-sharing strategies [8], and battery performance [9], reflecting the diverse aspects of this field. In [7], the authors compared different energy sources and determined that batteries emerge as the most promising solution for electric propulsion systems in ships, attributed to their higher energy and power density than other alternative energy storage solutions. Three distinct types of electrified ships are recognized in the literature: plug-in, hybrid, and full-electric ships [1]. Plug-in hybrid and hybrid ships incorporate a traditional diesel engine [10] and a battery. In hybrid ships, the battery is charged using excess energy from the engine and is employed to absorb load fluctuations. In plug-in hybrid ships, the battery is charged via the electrical grid and is exclusively utilized for designated actions such as port maneuvering [11].

On the other hand, a full-electric ship relies solely on a battery as its primary power source, which is charged by connecting to the electrical grid. Electric propulsion finds suitability in various ship types [12], including ferries, icebreakers, cruise ships, and drill ships [13]. In [14], the authors examined a ferry with a power system comprising diesel engines [10] and a battery primarily utilized for power supply during emergency maneuvering. Their investigation revealed higher efficiency of auxiliary engines, leading to reduced maintenance costs and increased engine lifetime. In [15], the authors investigated an offshore supporting ship propelled by diesel engines and equipped with a battery, showcasing reduced local emissions from the battery's integration. The launching of the Norwegian MF Ampere in 2015, the world's first battery-powered ferry, constituted a noteworthy milestone in advancing the electrification of maritime transport using power batteries [1].

Lithium-Ion Batteries (LIBs) have become the most popular type of batteries used in different electric energy storage systems due to their much higher energy density, higher power density, low self-discharge rate, and considerably greater lifecycles [16-17]. The main components of LIB include the cathode, anode, vent, electrolyte, separator, and terminals. The type of LIB is typically named after its cathode chemistry. For maritime applications, three prominent cathode chemistries are recognized: Lithium Nickel, Manganese Cobalt Oxide (NCM), Lithium Titanate Oxide, and Lithium Iron Phosphate (LFP). Among these, NCM is renowned for having the highest energy density. As a consequence, maritime companies that aim to achieve the most effective compromise in terms of efficiency and energy safety frequently select this approach. The capacity and power density of battery cells are the primary considerations when selecting one for short-sea transportation. This is a result of the fact that batteries must be able to manage the required acceleration during operations while sustaining sailing over comparably greater distances [7]. Battery material, the total amount of battery cycles, temperature during operation, charging and discharging C-rate, Depth of Discharge (DoD), and the number of charged/discharged cycles are some of the complicated variables influencing the performance degradation of LIB. Both the anode and cathode materials selected have an enormous impact on the way the battery operates and how fast it degrades based on operational conditions. As an example, batteries made from LFP have become prevalent in numerous types of vehicles because of their cost and durability, as well as thermal concerns.

LIB cells degrade over time, specifically during long storage time and repeated charge-discharge cycles. Various factors, such as operating temperature, the battery's State of Charge (SOC), and the charging or discharging current rate, significantly influence the rate of degradation. Higher temperatures and high charge-discharge rates accelerate the aging process, reducing the battery's overall lifespan and performance [17]. In particular, extreme temperatures could accelerate the breakdown by triggering unexpected chemical reactions within the cells, and extreme discharge and charge rates may result in unsafe lithium deposits [18]. Monitoring the battery's process of degradation is challenging despite the fact that it includes complicated electrochemical reactions. To correctly determine how long a battery can endure, all these factors must be taken into account [19]. Understanding the connections among components, production methods, and usage habits, therefore, becomes essential to developing accurate models that estimate LIB life over time. Although battery Remaining

Useful Life (RUL) prediction has been extensively studied in grid-scale energy storage, electric vehicles, and aerospace systems, maritime batteries exhibit unique degradation patterns because of their hybrid propulsion operating modes, high thermal variability, and irregular load cycling. Hybrid vessels frequently experience peak power demands during operations, especially during maneuvering and port operations, and as a result, unlike conventional vessels, degradation behavior becomes nonlinear. Because sufficient datasets on this topic are either unavailable or difficult to access in the maritime industry, creating and improving existing models requires time [20].

While many factors influence the energy efficiency and cost-benefit ratio of LIBs, a significant research gap exists in predicting the RUL of LIBs in hybrid vessels. This gap explicitly relates to the application of data-driven algorithms for accurate RUL estimation, which is important for enhancing operational reliability and optimizing maintenance schedules in maritime applications. Developing robust predictive models could help bridge this gap, offering insights into battery health and lifecycle management under the unique conditions faced by hybrid vessels. Despite the existence of studies in literature that predict the RUL of LIBs and employ various approaches, this specific area remains underexplored.

This study contributes to the literature by addressing the following aspects, which are different from previous works and add to the existing area of knowledge:

- The RUL of LIBs, a crucial component in hybrid vessels, has been predicted using data-driven algorithms for a hybrid vessel.
- By comparing several data-driven models with actual ship operating data, this study addresses the challenge of precisely predicting the RUL of LIB's, in contrast to earlier research that has primarily focused on energy management or fuel savings in hybrid ships.
- A comparative prediction process has been developed to thoroughly analyze the performance of data-driven algorithms in predicting the RUL of LIBs. A comparative analysis was also conducted with similar studies in literature.
- In the prediction study, nine algorithms used in similar problems in the literature were selected to examine the performance of data-driven algorithms, especially for this problem, and the algorithm parameters were optimized for performance.

The remaining sections of the study are structured as follows; the second section includes a comprehensive literature review of related studies in the field, and the third section covers materials and methodology. In the fourth section, the predictive analysis and comparative examination of algorithm scores are discussed, followed by the interpretation and discussion of the results obtained in the fifth and final sections.

2. Related studies

Due to the emission regulations that have come to the forefront in recent years, the issue of developing and using more efficient shipping systems has come to the front of the literature. In a study on this subject, the issue of LIBs on ship electrical networks and their types was discussed. In this research, a comparative analysis of a traditional drive system and a battery-driven system was carried out. As a result of the study, it was suggested that an approach carried out by ships with LIB is a more efficient and sustainable approach than the other approaches considered [1]. The study revealed that factors such as the propulsion system on the ship, voyage status, and fuel type directly affect the emissions generated during the voyage and the amount of fuel consumed. In this research, it has been suggested that in power-take-in mode, when the ship is close to the port, emissions can be significantly reduced thanks to the power obtained from auxiliary machines instead of the main engine. As a result of the study, it was determined that using LNG fuel with hybrid ships can reduce the amount of emissions from the ship and contribute significantly to energy efficiency [4, 21]. It has been stated that traditional ship propulsion systems no longer provide sufficient energy efficiency and that emission rates remain higher than in advanced ships in a study that examines how the climate brought on by environmental concerns in the maritime industry has accelerated the transition to hybrid ships and electric ships and that studies in this field have begun to come to the front in the literature. An energy management system was developed for research, and it was stated that this system may lower emissions [5]. A study that

examines the significant potential for emissions reductions from ships with hybrid propulsion and battery systems in ports has stated that hydrogen-based fuel supply and more easily accessible access to power in the port are beneficial developments. This study examined the construction of a passenger ship with a hybrid propulsion system and its reinforcement with battery systems. It was discovered that the dynamic programming methodology can identify sudden power changes on board the ship with high accuracy, owing to reinforcement learning [6]. According to a study, there may be negative environmental repercussions from increased maritime activity worldwide. As indicated, the IMO has established strict rules to prevent greenhouse gas emissions. Such regulations have increased energy efficiency practices on ships. Thanks to the applications made, alternative propulsion systems on ships have been addressed in various research and development processes. Ship propulsion systems with electric and hybrid propulsion provide an important opportunity for reducing pollution. The results of the study suggested that by including alternative powering technologies, alternative fuels, and rechargeable batteries, vessels using conventional power systems could substantially decrease their negative environmental impact [7]. As part of the research on the utilization of renewable energy systems on the ship, the main and auxiliary energy structures of a cruise vessel have been designed and assessed. The research determined the power demand of the vessel over multiple voyage conditions. Study utilizing simulation followed in connection with the predicted power demand. The study's findings have led to the determination of the potential power that can be generated by solar energy, fuel cells, and the diesel generator set installed on the ship, as well as the potential emissions. In the future, employing solar energy and batteries on ships rather than fossil fuels can considerably lower emission rates [8]. Battery systems and electric propulsion have become indispensable and relevant, particularly in ships performing short-range excursions, according to a study that suggests incorporating battery systems into ships can prevent emissions. Batteries and electrically powered ships may have significant development potential in the maritime industry because of the battery management system developed in this study [9]. According to an investigation that declares integrating battery systems into vessels assists in reducing GHG emissions, battery systems, and electrical propulsion have become crucial and relevant, particularly for vessels performing short-range voyages. Due to the battery control system developed during this study, the maritime industry may see enormous expansion of the use of batteries and electric-powered vessels. As a result of the study, dual-objective optimization is much more functional than single-objective optimization studies and can potentially be used in the future [11]. It was demonstrated that hybrid designs are significantly more environmentally friendly than conventional methods in an investigation that discussed how hybrid design structure has recently developed into a vital development and research procedure for commercial vessel operations. The research investigation suggests that vessels using hybrid engine technologies may rapidly reduce fuel consumption by up to 20 %. Given its likelihood of becoming thoroughly used, implementing a hybrid technique in autonomous vessels has been assessed as a field with future potential [13]. A study analyzed the integration of the battery system for a conventional diesel-powered ship. This analysis study examined data obtained from a ship operating a short-range voyage in the Baltic Region. While analyzing the battery installation cost, it was evaluated that it would be more beneficial to first undergo an optimization process for the main engine and auxiliary machines on the ship. Additionally, it has been determined that the installation of the battery system has the potential to reduce the vessel's annual GHG emissions by approximately 250 tons [10]. The results of the research revealed that hybrid engines on vessels had a lot of potential as a technique for decreasing pollution [14]. Ships used to support offshore platforms have become essential in recent years as the oil industry turns to subsea resources. Due to critical safety measures and emission restrictions on such ships, hybrid ships and electric propulsion ships may be an alternative solution. A study conducted in this field determined that the combination of the classical internal combustion propulsion system and battery technology will become much more common in the coming years. The research presented the need for studies on the lifespan of batteries as an area that should be investigated in the coming years [15]. The electrically powered operation of vessel energy systems has become essential due to attempts to decrease pollution and implement maritime authority. Based on a study in this domain, battery storage technology plays an important part in improving vessel energy efficiency. The research additionally illustrates the potential of increasing ship efficiency in energy with alternate energy sources [7]. The demand for alternative energy sources has brought attention to the battery problem in recent years. The value of batteries has grown as electrical technologies

have replaced internal combustion engines in many applications. A study estimated the remaining lifetime of batteries. There has been a contention that machine learning techniques can be a viable substitute for artificial neural networks in prediction tasks due to their alleged inferior performance. The study used a 40-cycle dataset, and the average absolute error of the forecast was about 11 % [19]. An investigation which employed a digital twin methodology for modelling vessel cranes in the maritime sector studied the model in a number of scenarios and produced favorable results. It was stated, according to the findings of the research, that a digital twin methodology may be effectively applied to identify potential risks and assess optimal operating conditions for cranes [22]. The importance of data-driven studies has increased in the maritime sector in recent years. Chen et al. (2025) claimed that the SOH and RUL values of LIBs can be calculated using single cycle charging data [20]. Furthermore, in another study, Meng et al. (2025) designed an early warning system for dual-fuel ships, utilizing deep learning methodology [12]. While there have also been studies in explainable artificial intelligence on this topic, Hoang et al. (2025) proposed a methodology for estimating fuel consumption from operational data [10]. Using a fault detection methodology for ship components, Su et al. (2024) argued that ship health monitoring could contribute to energy efficiency and emissions reduction [21]. In addition to these studies, Liu et al. (2024), in a study using the digital twin approach to model cranes on ships, stated that the reliability of crane systems on ships could be increased through the digital twin method [22].

3. Materials and methods

3.1 Ship power plant and battery dataset

This study considers a cargo ship with a hybrid power plant used for commercial purposes for a North European shipping company. Various parameters of the ship are listed in Table 1. The vessel power plant architecture is given in Figure 1. As shown in Figure 1, the vessel has one main engine, three generators, one emergency generator, and a battery system. The features of the statistical summary of the ship's battery system dataset are given in Table 2 and the correlation matrix for the dataset is shown in Figure 2. The battery pack consists of series-parallel modules of lithium-ion cells with NCM chemistry. The initial nominal cell capacity was 100 Ah, and the rated capacity is 1 MWh. Prior to data collection, the system had been operating for about two years, with a typical DOD of about 80 %. When the pack's usable capacity fell below 70 % of its nominal value, it was retired. The dataset was collected during the hybrid vessel's regular operational trips, ensuring that the measurements accurately reflect loading and discharging conditions. Raw onboard measurement data were preprocessed to ensure reliability and remove noise-related artifacts before model training. Due to transmission problems, cycles with missing voltage or current values were eliminated. A Savitzky-Golay smoothing technique was used to filter high-frequency measurement noise to try to eliminate signal spikes and maintain electrochemically significant trends. Using z-score analysis, outliers resulting from anomalous operational events were found and eliminated when $|z| > 3$ for cycle duration, minimum voltage, or maximum discharge values. To make sure that charge and discharge intervals were consistent across samples, each cycle was divided using characteristic voltage transition points after filtering. The parameters were normalized using min-max scaling system to avoid feature supremacy and provide a trustworthy infrastructure for comparing algorithms. By using these preprocessing methods, battery degradation patterns during hybrid vessel operations were reliably and accurately represented in the processed dataset.

The LIB pack, installed on the ship studied in this study, was designed to support power sharing between the diesel generators in the ship's power scheme. It provides support such as auxiliary power during low-speed operations, temporary load smoothing during acceleration, and peak shaving during maneuvering. Therefore, the primary cause of battery degradation observed in the dataset is real voyage conditions rather than laboratory conditions. Therefore, the battery aging factor under various realistic, ship-specific power demand models is reflected in the estimated RUL in the study.

Table 1 Analyzed ship parameters

Type of the ship	General cargo
Deadweight Tonnage (DWT)	5400 mt
Length	90 m
Breadth	16 m
Draft	6.3 m
Gross Tonnage (GT)	4150
Net Tonnage (NT)	2200
Built year	2023
Main engine	1920 kW
Battery pack	1 MWh
Generator set	3x350 kW
Emergency generator	1x350 kW

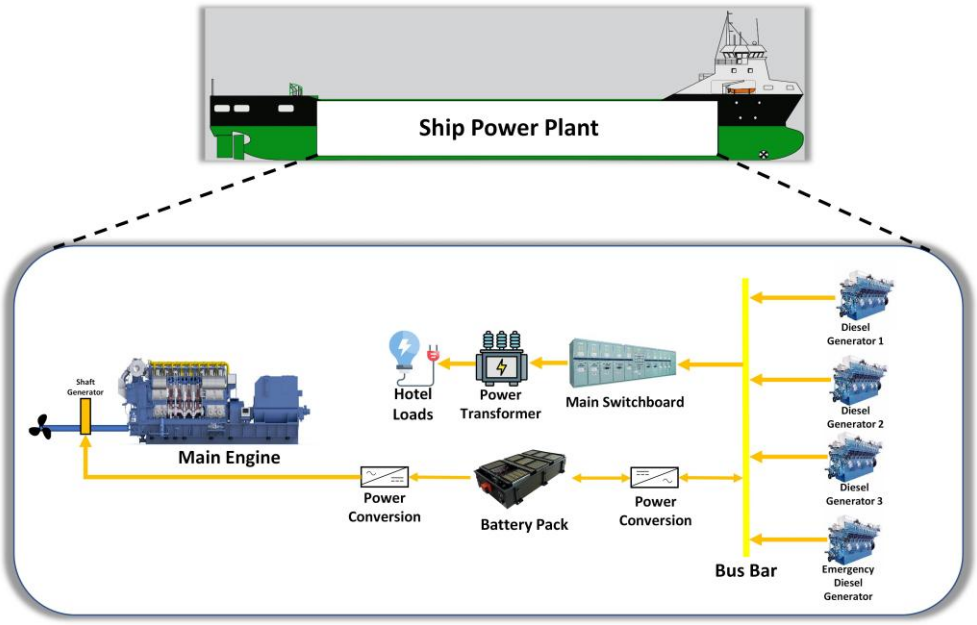

Fig. 1 Outline of a ship power plant and its basic components. The system includes the main engine for propulsion, generators supplying electricity to onboard systems, and Battery Energy Storage System (BESS) for hybrid vessels

Table 2 Statistical analysis of the battery dataset

	Cycle index	Discharge time (s)	Decrement 3.6-3.4V (s)	Max. voltage discharge(V)	Min. voltage charge (V)	Time at 4.15V (s)	Duration of constant current stage (s)	Charging time (s)	RUL
Count	13761	13761	13761	13761	13761	13761	13761	13761	13761
Mean	563.37	4515.7	1159.7	3.9	3.58	3717.68	5393.78	10031.72	546.8
Std	319.77	33074.47	14529.19	0.0917	0.1235	8982.74	25177.11	26344.71	319.88
Min	1	8.7	-397544.5	3.043	3.022	-113.58	5.98	5.98	0
25 %	284	1164	317.2	3.843	3.493	1813.36	2528.38	7853.5	273
50 %	569	1542.12	433.2891	3.903	3.577	2876.343	3752.34	8322.31	542
75 %	837	1893.12	592	3.97	3.664	4033.191	4976.32	8756.34	826
Max	1134	958320.3	406703.7	4.36	4.37	245111.12	880728.1	881008.2	1134

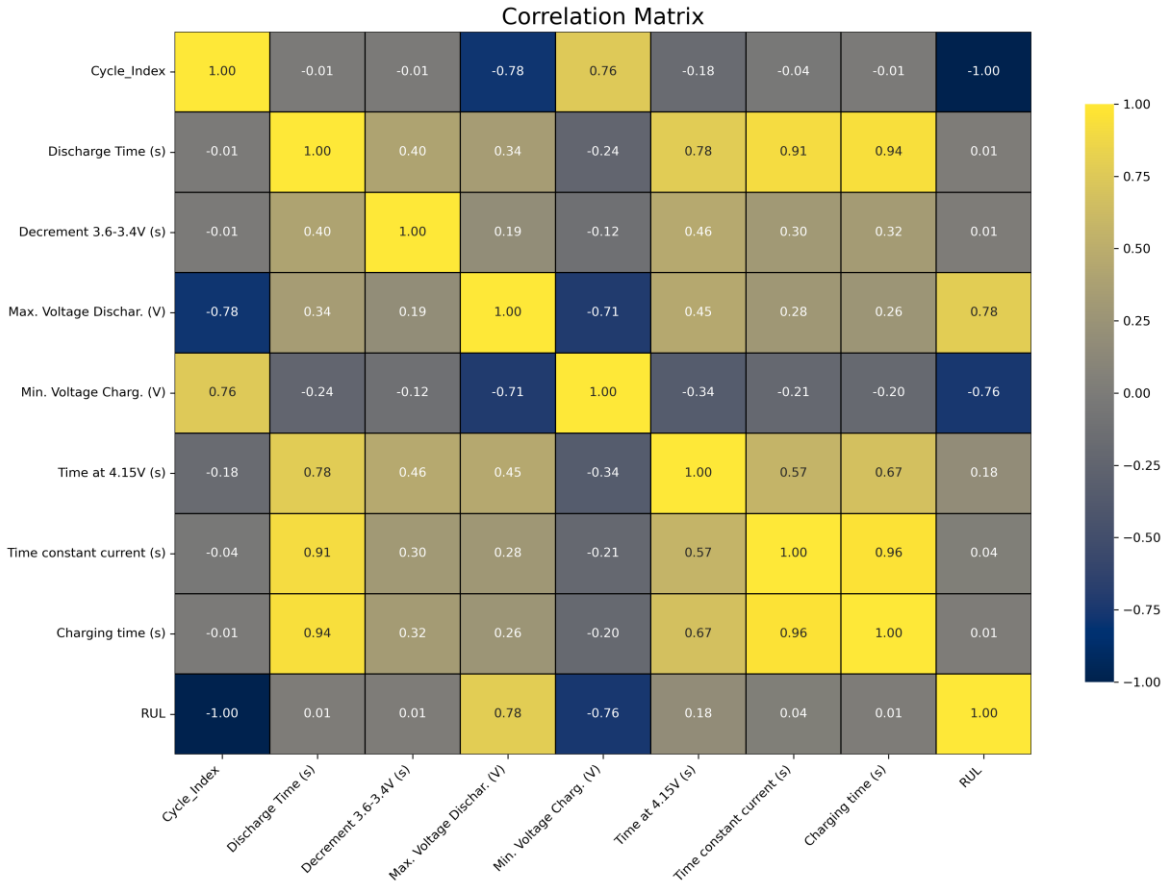

Fig. 2 Pearson correlation matrix of the dataset

The dataset includes samples where the battery's functional capacity drops below 80 % as well as the battery's entire operational life. The typical knee-point behavior, in which degradation accelerates quickly and nonlinearly, is seen in these late-life cycles. For the purpose of assisting the models learn both gradual and accelerated degradation regimes and better represent real-world LIB aging in maritime applications, these cycles were kept rather than eliminated. Duration of constant current stage (s) is a column that indicates how long the battery runs under a constant-current discharge scenario. Since constant-current portions provide trustworthy electrochemical information that has a strong connection to the evolution of internal resistance and capacity decrease, this stage was extracted.

3.2 Data-driven algorithms

In this study, nine different data-driven approaches were used to estimate the RUL of the battery system of a commercial container ship equipped with a hybrid power plant. The relevant methods are explained in detail below.

3.2.1 Multiple-linear regression

The Multiple-linear regression method, a classic algorithm frequently used in statistical analysis and data science, searches to find the dependent variable using independent input variables [23]. In other words, this algorithm can produce realistic results in cases where a linear relationship can be established between the dependent variable and independent variables [24]:

$$A = B_0 + B_1X_1 + B_2X_2 + \cdots + B_NX_N \tag{1}$$

In Equation (1) A is the dependent variable, ε is the error, X variables can be expressed as independent variables, and B values can be expressed as coefficient values [25]. In this equation, values B are calculated as:

$$A_N = \text{argmin}_{(B)}^{(\sum_{i=1}^{N} A_i - B_0 - (\sum_{j=1}^{N} B_j x_{ij})^2)} \tag{2}$$

3.2.2 K-Nearest Neighbors (K-NN)

The K-NN method has become popular for determining the nearest neighbors of a certain point [25]. In this algorithm, the k parameter varies according to the model created. Based on past data, the algorithm calculates which neighborhood the new point belongs to. Minkowski distance (L^P) is one of the most critical parameters in the algorithm and is used to calculate the margin between a point (x_q) and another point (x_j) [26]:

$$L^P(x_j, x_q) = (\sum_i |x_{j,i} - x_{q,i}|^p)^{1/p} \tag{3}$$

In Equation (3), when the p-value is accepted as 1, the Manhattan distance is obtained, and when the p-value is 2, the Euclidean distance value is obtained [27].

3.2.3 Extreme Gradient Boosting (XGB)

The XGB algorithm, which is a hybrid version of the Decision tree and Gradient boosting methods, uses the values obtained by summing the results obtained by the Decision tree method in the first stage [27]. This value is calculated as follows:

$$\hat{y}_i = \sum_{k=1}^{N} f_k(x_i) \tag{4}$$

The XGB algorithm, which applies a penalty in the case of complexity and thus aims to optimize the loss function, tries to converge to its target by improving the objective function [28]. In this structure, the loss function (LF) is shown in Equation 5, and the complexity penalty (CP) is shown in Equation 6:

$$LF = \sum_{i=1}^{N} l(y_i, \hat{y}_i) \tag{5}$$

$$CP = \sum_{k}^{k} \Omega(f_k) \tag{6}$$

3.2.4 Support Vector Machines (SVM)

The SVM method was developed by Bell Labs and has been frequently used and widespread in data-driven problems [29]. The support vector machine, a highly effective technique, gives consistent results in classification and regression problems. In the support vector machine method, the points between a certain number of support vectors and the predictions falling within this range are considered successful. In contrast, the region outside this range is considered unsuccessful. In classification problems, support vectors are structures that determine the boundaries between classes [30]. The equations related to support vectors are shown below:

$$f(x) = w^T x + w_0 \tag{7}$$

$$H(w, w_0) = \sum_{i=1}^{N} (y_i - f(x_i)) + \frac{\lambda}{2} \|W\|^2 \tag{8}$$

$$V_{\in}(r) = \begin{cases} 0 \ \ if \ \ |r| < \in \\ |r| - \in \ \ otherwise \end{cases} \tag{9}$$

where x represents the independent variable, w is the normal vector. Also, λ is the alignment parameter, w_0 is a constant number. V is the error function, $\mathcal{E}$ is the error margin, and r is the error value [31].

3.2.5 Random forest

Random forest, an ensemble learning method, is a classic algorithm that has successfully solved problems such as regression and classification for years [32]. In this method, while finding the result, unlike the decision tree method, the average of the trees from which the results are taken gives the obtained result. In this way, the random forest method overcomes the overfitting problem in the decision tree method. Another aspect of this method is that it is extremely robust against adding irrelevant features [33].

In this method, when $X = x_1, x_2, ..., x_n$ is given as input and training set and $Y = y_1, y_2, ..., y_n$ is given as output values.

If $c=1,2,..., C,$ the number of examples (n) consisting of X and Y values are called X_c and Y_c, and the regression tree (f_c) is trained on X_c and Y_c; the prediction process performed after training is calculated by taking the average of individual results found by each tree (x') is below [34]:

$$F' = \frac{1}{C}\sum_{c=1}^{C} f_c(x') \tag{10}$$

The standard deviation value for the predictions from each individual tree at x' can be found with the following equation:

$$std = \sqrt{\frac{\sum_{c=1}^{C}(f_c(x') - F')^2}{C-1}} \tag{11}$$

3.2.6 Ridge

This algorithm is developed to perform coefficient estimation using the least squares method [35]. The following equation shows the coefficient (a_x) calculation process:

$$a_x = \operatorname{argmin}_{(a)}^{(\sum_{i=1}^{x}((y_i - a_0 - \sum_{j=1}^{D} a_j x_{ij})^2 + r\sum_{j=1}^{D} a_j^2)} \tag{12}$$

If the equation above is examined, it means the regularization parameter, with the r value being greater than zero [36].

3.2.7 Lasso

In this method, a variable selection process is performed using the least squares method. In the process of finding the coefficient (a_x), the least squares method is used, and the equation developed for finding the coefficient is shown below [37]:

$$a_x = \operatorname{argmin}_{(a)}^{(\frac{1}{2}\sum_{i=1}^{x}((y_i - a_0 - \sum_{j=1}^{D} a_j x_{ij})^2 + (r\sum_{j=1}^{D}|a_j|))} \tag{13}$$

3.2.8 Elastic net

In the Elastic net method, which uses the regularization parameters of Ridge and Lasso methods, the hyperparameters (a and rl_{ratio}) of the algorithm are found with the equations below [38]:

$$a = r_{Ridge} + r_{Lasso} \tag{14}$$

$$rl_{ratio} = \frac{r_{Lasso}}{a} \tag{15}$$

3.2.9 Long Short Time Memory (LSTM)

LSTM algorithm is a Recurrent Neural Network (RNN) that aims to alleviate the vanishing gradient problem encountered in classical RNNs. It provides a short-term memory for RNN containing many time steps, so it is called LSTM [39]. The LSTM structure generally consists of three gates and one cell. These gates are called the input gate, the output gate, and the forget gate. The cell structure is a subsystem that

remembers values at random intervals, and the gates are responsible for regulating the flow of information entering and exiting the cell. The input gate is responsible for selecting new pieces of information to store in the current cell state, while the forget gate determines which information to discard [40]. The LSTM algorithm was used in this study to compare and analyze the performance of classical algorithms with a more innovative and modern algorithm compared to other algorithms.

3.3 Validation and evaluation

Three different error metrics were used to quantify the values obtained in the estimation study carried out during the simulation process and compare the algorithms with each other in more detail. The K-fold cross-validation method was used to verify the study results [41]. To ensure reliability of the evaluation between models, a 5-fold cross-validation method was used. 60 % of the samples were used for training, 20 % for validation, and 20 % for testing. Data leakage was prevented during the training and testing phases by processing the data so that they did not overlap. Although the dataset used in this study was taken from the same vessel, this method allowed the model performance to demonstrate its predictive ability on unseen operational variables.

3.3.1 K-fold cross-validation

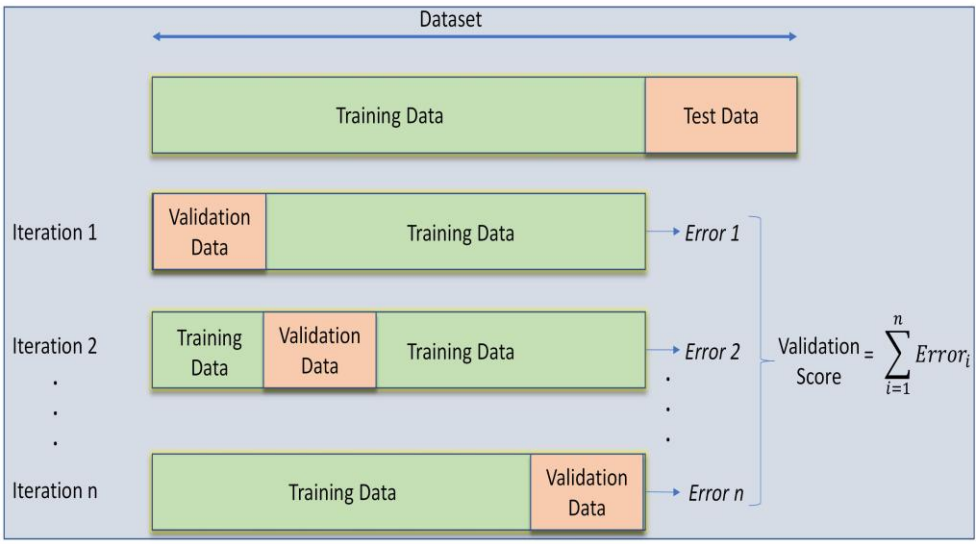

Fig. 3 K-fold cross-validation process

In data-driven methods, the K-fold cross-validation method is used at the end of the problem-solving process to determine whether the algorithms have an overfitting problem [42]. This study divided the dataset into five equal sample sets. One of these sets was separated for validation, the other one was separated as the test set, and the remaining three sets were used as training data to perform the cross-validation process [43]. The process continued until all the samples in the dataset were scanned. After all the samples in the dataset were scanned, the process was terminated, and the average of the obtained scores was taken as the validation score. The K-fold cross-validation score is given in the Equation (16). In this equation, Ɛ represents the error value for each iteration:

$$Validation\ score = \sum_{i=1}^{n} \varepsilon_i \tag{16}$$

The K-fold cross-validation process is illustrated in Figure 3 [44].

3.4 Error metrics

3.4.1 Mean Absolute Error (*MAE*)

In data-driven problems, the calculation of the average of the absolute values of the distance between the actual values in the dataset and the values predicted by the algorithms is found with the error metric called *MAE*. The calculation process of the *MAE* is given below [45]:

$$MAE = \frac{1}{n}\sum_{j=1}^{n} error_j \tag{17}$$

where, $error_j$ shows the absolute value of the distance between the dataset's actual values and the algorithms predicted values [46].

3.4.2 Root Mean Squared Error (*RMSE*)

In data-driven problems, the distance of the predictions made by the algorithms to the real values in the dataset is determined by the error metric called *RMSE*. The calculation process of the *RMSE* is shown below [47]:

$$RMSE = \sqrt{\frac{\sum_{j=1}^{n} error_j^2}{n}} \tag{18}$$

In this equation, the $error_j$ value is the difference between the actual value in the dataset and the predicted value. The value of n represents the amount of data [48].

3.4.3 Coefficient of Determination (R^2)

R^2 can be explained as the predictable ratio of the variation in the dependent variable from the independent values in data-driven problems. It allows the model's success to be measured and quantified from the total variation of the results obtained by the algorithm. The equation for the calculation of R^2 is given below [49]:

$$R^2(V_a, V_p) = 1 - \frac{\sum_{j=1}^{n}(V_{aj} - V_{pj})^2}{\sum_{j=1}^{n}(V_{aj} - k)^2} \tag{19}$$

where, V_a is actual value, V_p represents the predicted value, and k represents the mean of the actual values [50].

4. Simulation results and discussion

The simulation study was developed using the 3.7.7 version of the Python programming language using the Tensorflow environment, and the relevant studies were carried out using the Spyder 4.0 interface [51]. When the simulation was run with the default algorithm parameters, it was determined that some methods did not give the desired results and were inefficient in the battery's RUL prediction process. When the relevant parameters were optimized, and the simulation was rerun, it was observed that the efficiency of the algorithms increased. Simulation results with the default parameters of algorithms and their optimized versions are shown in Table 3. The results of the K-fold cross-validation process are shown in Table 4. The updated parameter values of the algorithms after the optimization process are shown in Table 5. Simulation results for the prediction of the battery RUL for the hybrid ship are shown in Figures 4-21. For all simulation figures (Figures 4-21), the horizontal axis represents the cycle index, corresponding to the sequential numbering of battery operating cycles over time. The vertical axis represents the RUL expressed in cycles. The true degradation trajectory obtained from operational data is denoted by "Actual RUL" in each plot, whereas the other curves show model predictions both before and after hyperparameter optimization. These explanations are given here to prevent duplication because all figures use the same axis definitions and labeling conventions.

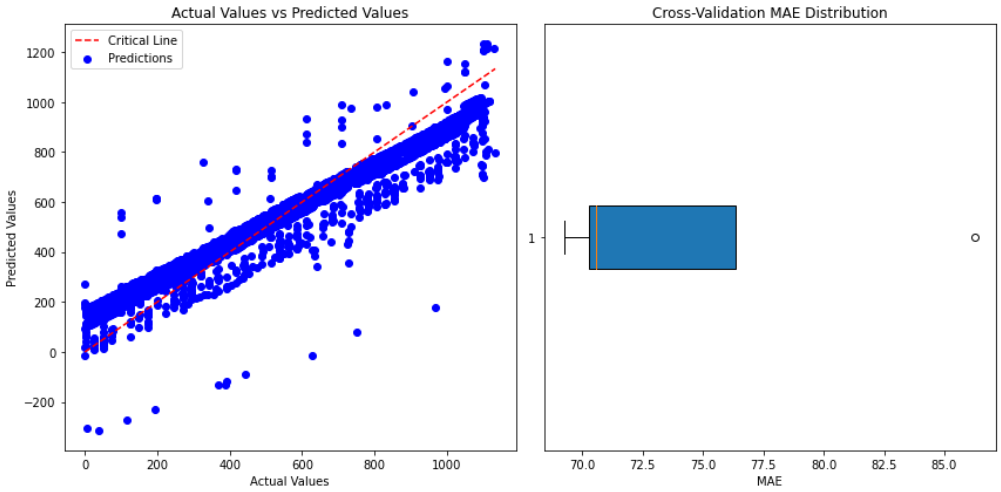

Fig. 4 Simulation results of the Elastic net algorithm before hyperparameter optimization

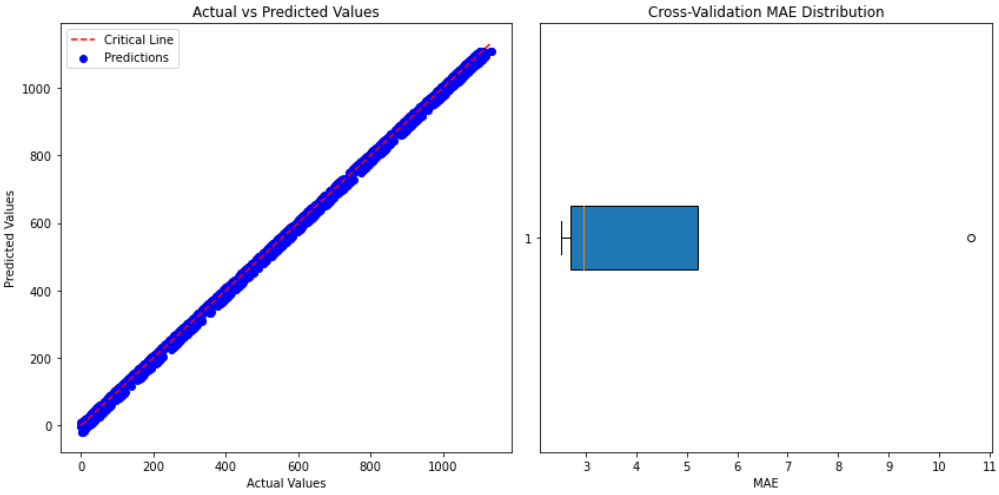

Fig. 5 Simulation results of the Elastic net algorithm after hyperparameter optimization

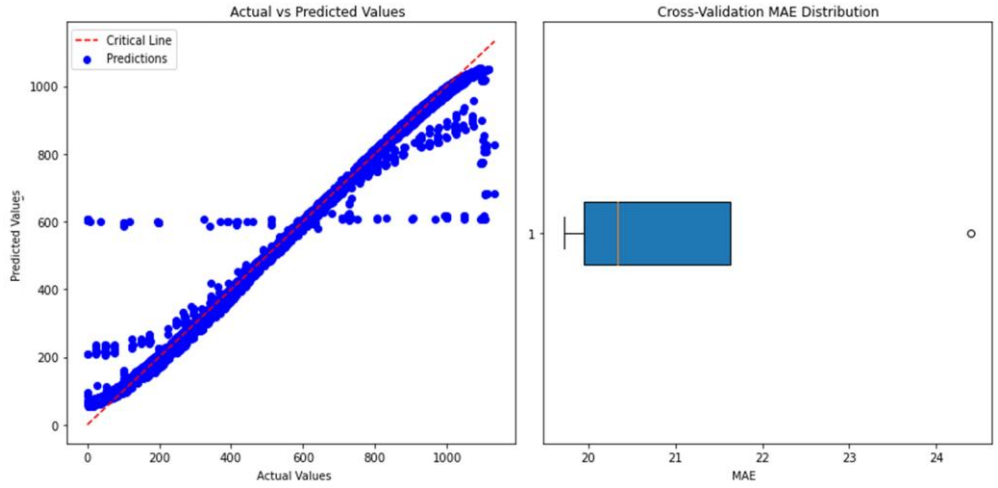

Fig. 6 Simulation results of the SVR algorithm before hyperparameter optimization

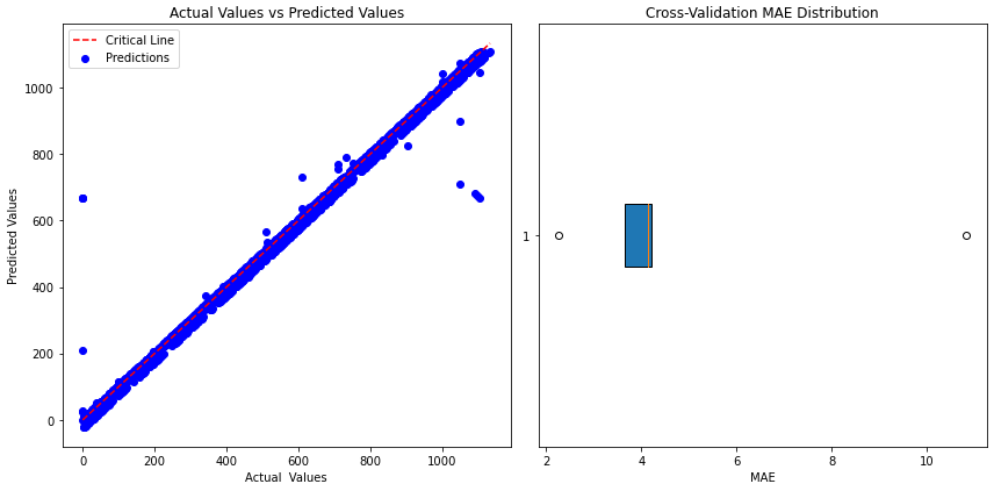

Fig. 7 Simulation results of the SVR algorithm after hyperparameter optimization

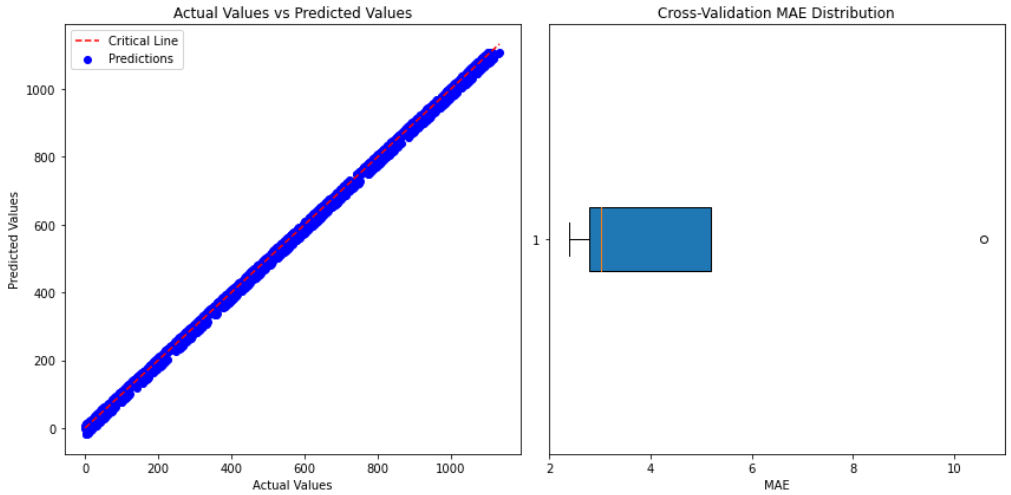

Fig. 8 Simulation results of the Lasso algorithm before hyperparameter optimization

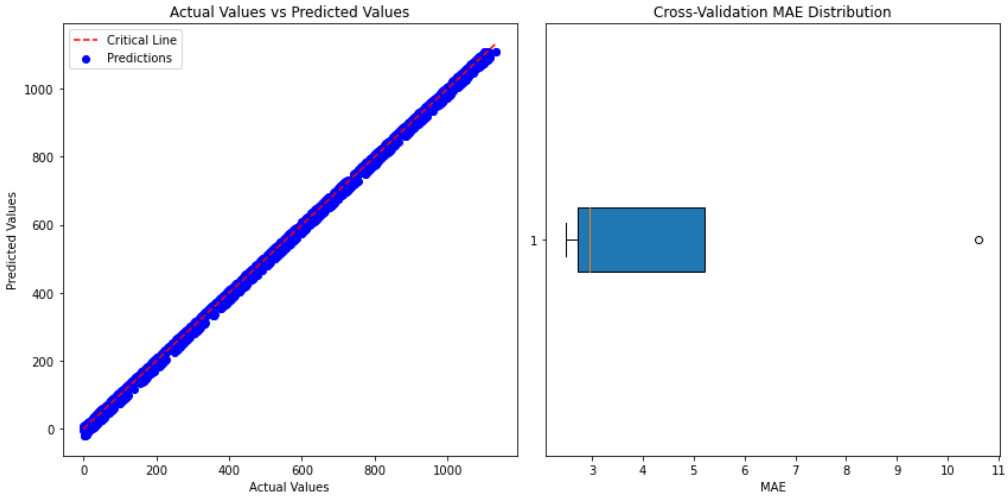

Fig. 9 Simulation results of the Lasso algorithm after hyperparameter optimization

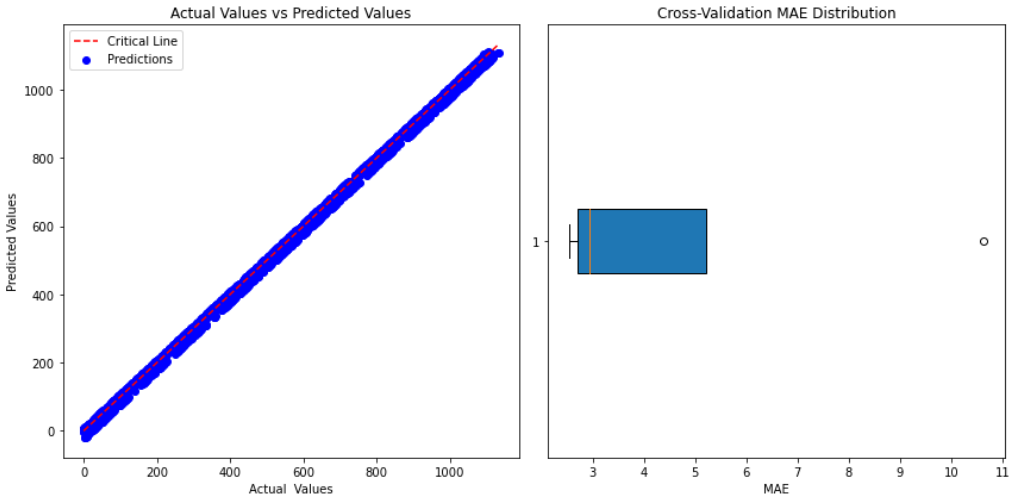

Fig. 10 Simulation results of the Ridge algorithm before hyperparameter optimization

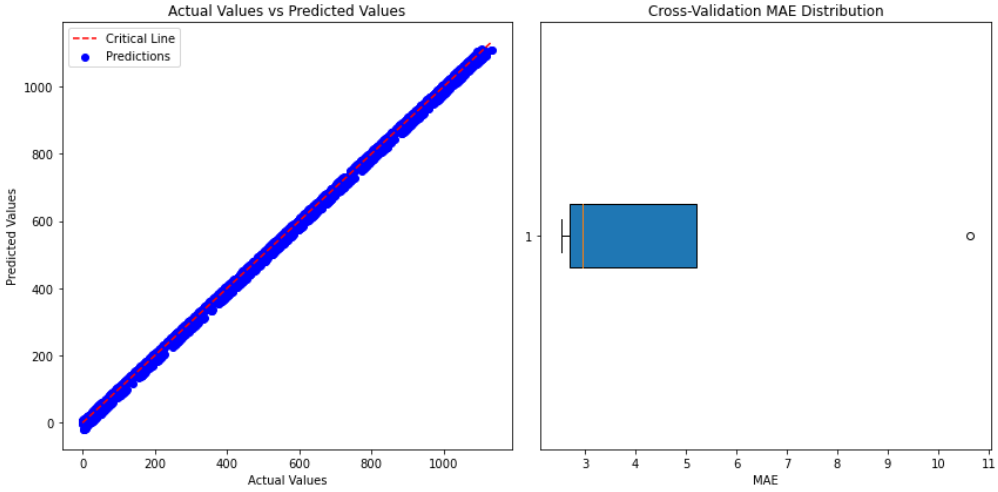

Fig. 11 Simulation results of the Ridge algorithm after hyperparameter optimization

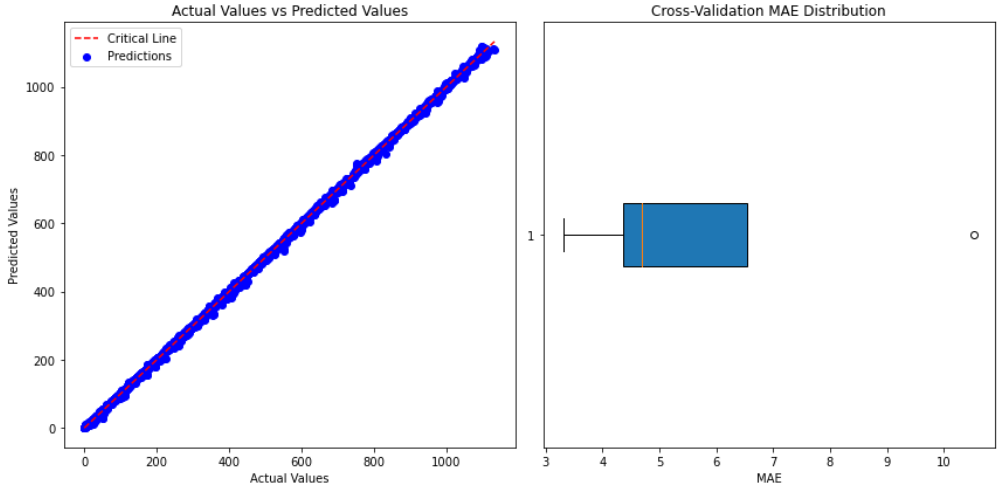

Fig. 12 Simulation results of the Random forest algorithm before hyperparameter optimization

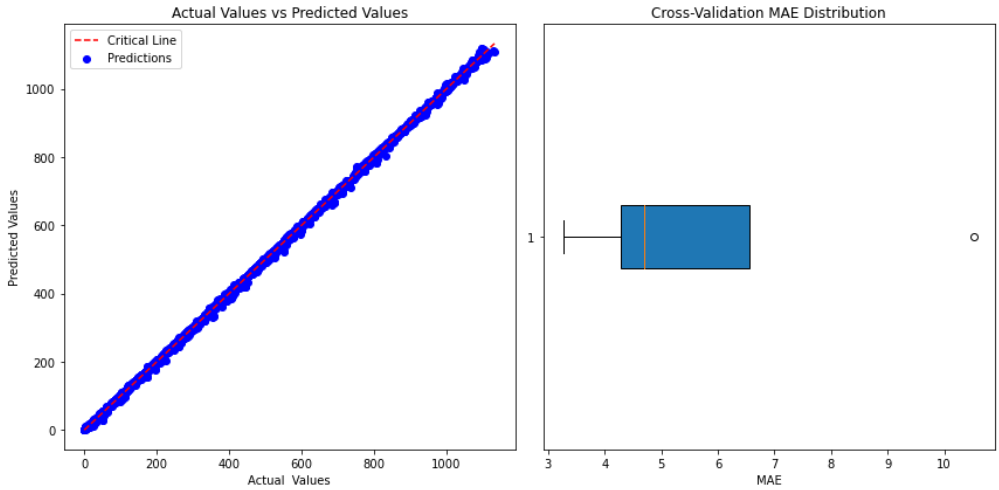

Fig. 13 Simulation results of the Random forest algorithm after hyperparameter optimization

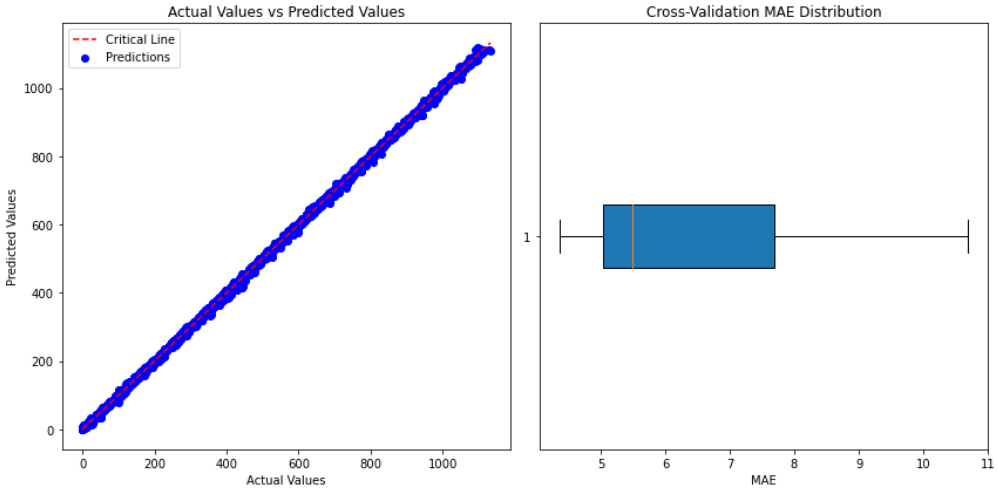

Fig. 14 Simulation results of the XGB algorithm before hyperparameter optimization

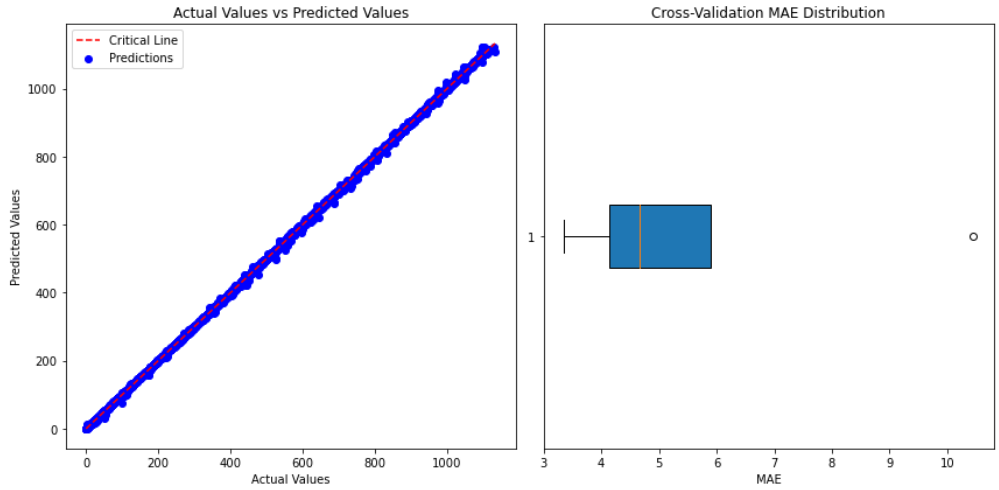

Fig. 15 Simulation results of the XGB algorithm after hyperparameter optimization

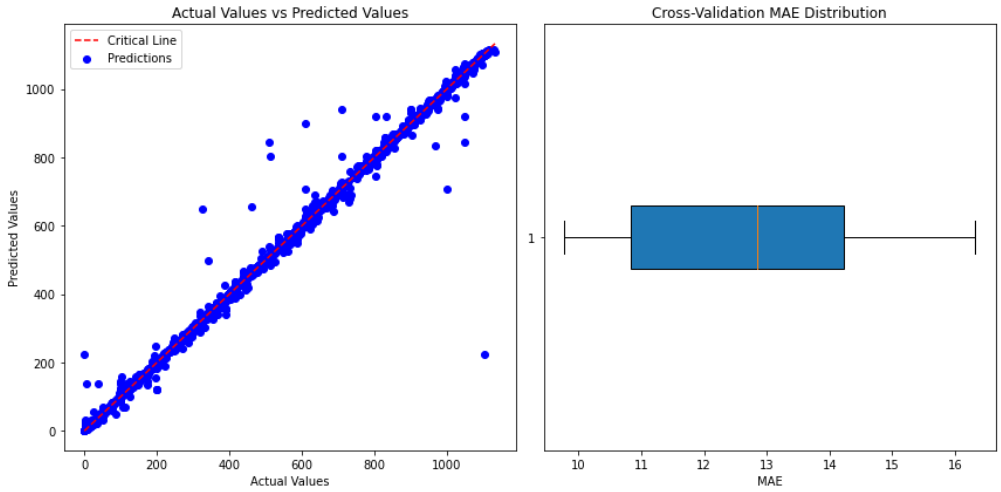

Fig. 16 Simulation results of the K-NN algorithm before hyperparameter optimization

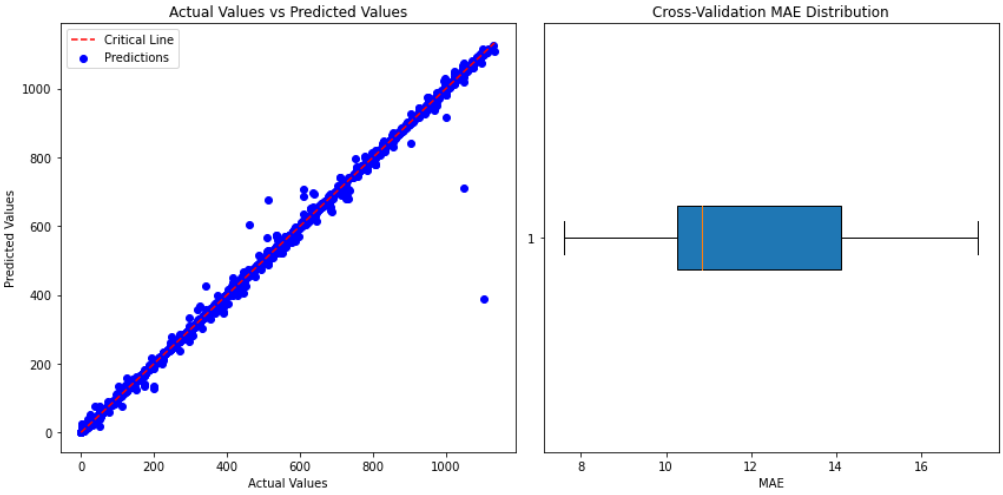

Fig. 17 Simulation results of the K-NN algorithm after hyperparameter optimization

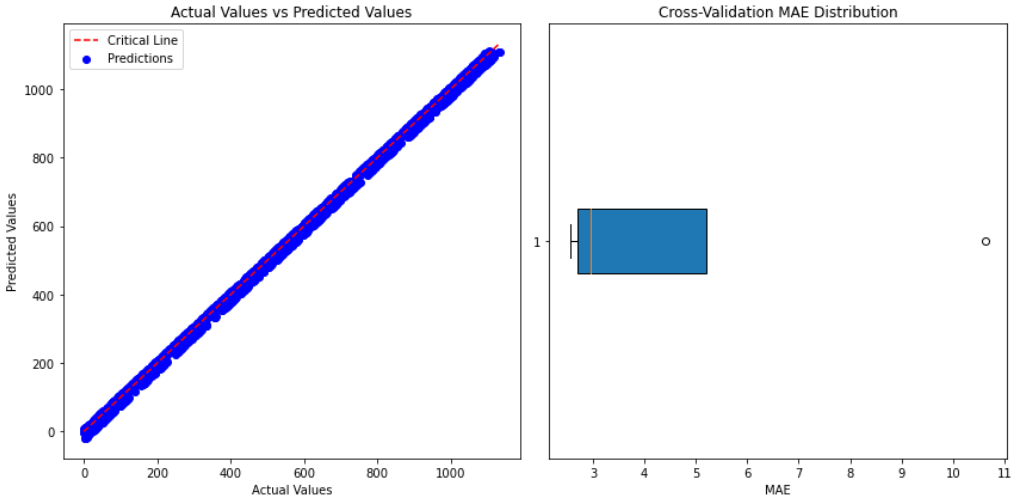

Fig. 18 Simulation results of the Multiple-linear regression algorithm before hyperparameter optimization

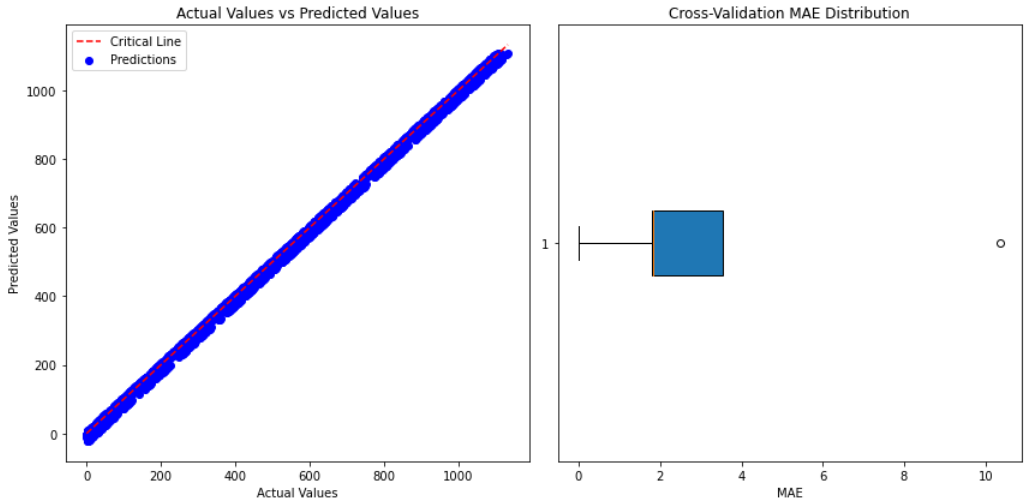

Fig. 19 Simulation results of the Multiple-linear regression algorithm after hyperparameter optimization

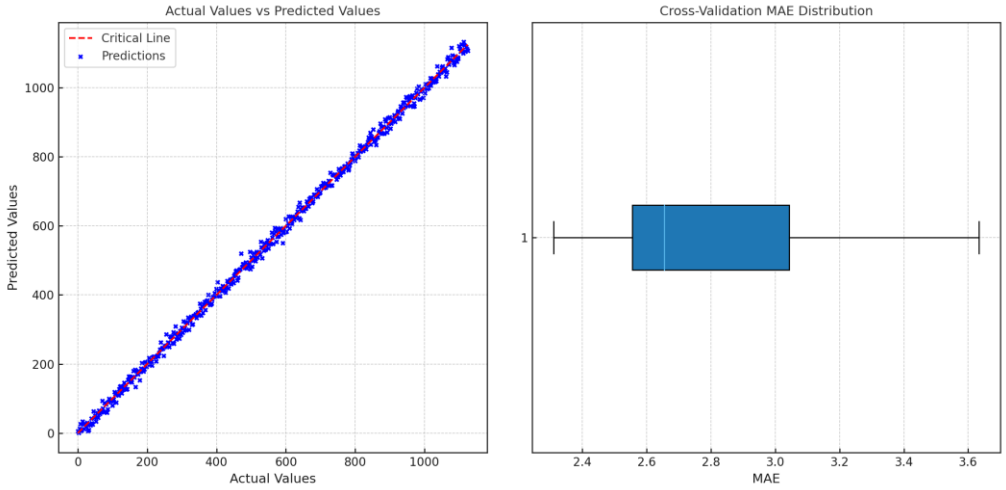

Fig. 20 Simulation results of the LSTM algorithm before hyperparameter optimization

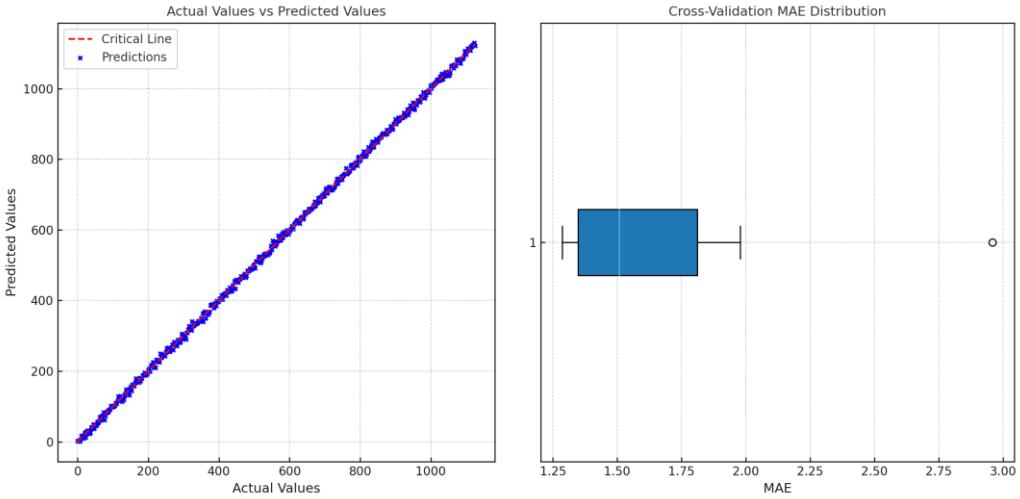

Fig. 21 Simulation results of the LSTM algorithm after hyperparameter optimization

When Figures 4 and 5 are compared, it is seen that there is a significant increase in the algorithm estimation performance after the parameter optimization process for the Elastic net algorithm. The mean absolute error can be significantly reduced. When Figures 6 and 7, which include the performance graphs for the support vector regression algorithm, are examined, it can be observed that the algorithm performance has

increased significantly after the optimization process. While the mean absolute error value was in a wide range, it was squeezed into a narrow range after the optimization process. When Figures 8 and 9, which include the graphs for the Lasso algorithm, are examined, the increase in the algorithm performance can be understood from the decrease in the mean absolute error value. It is observed from Figures 10 and 11, where the Ridge algorithm is considered, that there is no visible increase in the algorithm performance. When the simulation results of the Random forest algorithm are examined, it is seen that the algorithm performance does not increase significantly before (Figure 12) and after (Figure 13) the optimization process. When Figures 14 and 15, which include the XGB algorithm, are examined, it can be said that the algorithm performance has increased, especially over the mean absolute error value. When Figures 16 and 17, where the K-NN algorithm is discussed, are examined, it is observed that the prediction success can be improved after the optimization process. When Figures 18 and 19 are examined, it can be observed that the prediction success of the Multiple-linear regression algorithm increases with the optimization process. The LSTM algorithm's predictive performance both before and after parameter optimization is shown in Figures 20 and 21. The outcomes unequivocally show a significant improvement after optimization. A considerable drop in both *RMSE* and *MAE* values suggests a higher degree of predictive accuracy.

Table 3 Error metrics comparison for nine implemented algorithms, showcasing performance before and after hyperparameter optimization.

Algorithm	***RMSE***		***MAE***		***R^2***	
	Before	After	Before	After	Before	After
Elastic net	8829.33	50.61	74.221	4.5165	0.9149	0.9995
SVR	3315.67	519.60	21.701	4.4823	0.968	0.9949
Lasso	51.6022	50.6153	4.5337	4.52	0.9994	0.9995
Ridge	60.6298	50.6321	4.5294	4.5184	0.9994	0.9995
Random forest	15.3548	15.1739	2.2283	2.2053	0.9998	0.9998
XGB	18.6706	9.9068	2.9223	1.7308	0.9998	0.9999
K-NN	390.03	190.371	4.2968	2.9759	0.9962	0.9981
Multiple-linear r.	55.9837	50.6301	4.5205	3.4814	0.9994	0.9995
LSTM	12.573	6.337	2.8702	1.4591	0.9998	0.9999

Table 4 K-fold cross-validation results

	Fold 1		**Fold 2**		**Fold 3**		**Fold 4**		**Fold 5**		**Average Result**	
	Before	After	Before	After	Before	After	Before	After	Before	After	Before	After
Elastic net	70.5792	2.4992	70.3001	10.6332	69.2681	5.2150	86.2663	2.9477	76.3290	2.9477	74.5485	4.7988
SVR	19.7176	3.6592	24.3966	10.8283	21.6295	4.1346	19.9570	2.2665	20.3332	4.2116	21.2068	5.0201
Lasso	2.3955	2.4902	10.5890	10.6133	5.1987	5.2067	3.0145	2.9481	2.7848	2.7058	4.7965	4.7928
Ridge	2.5291	2.5390	10.6419	10.6382	5.2129	5.2115	2.9478	2.9461	2.7064	2.7058	4.8081	4.8076
R. forest	3.3229	3.2759	10.5260	10.5251	6.5360	6.5640	4.6941	4.7026	4.3656	4.2783	5.8889	5.8692
XGB	5.0407	4.6591	10.6883	10.4490	7.6841	5.8932	4.3668	3.3539	5.4936	4.1413	6.6547	5.6993
K-NN	12.8536	10.8481	14.2207	14.1217	10.8396	10.2660	9.7772	7.6078	16.3165	17.3383	12.8015	12.0364
Multiple-l. r.	2.5488	1.7936	10.6346	10.3611	5.2100	1.8346	2.9444	0.0086	2.7052	3.5381	4.8086	3.7052
LSTM	2.5421	1.6025	3.1978	1.3816	2.7643	1.4937	3.0564	1.4168	2.7903	1.4009	2.8702	1.4591

When the error metric values, as illustrated in Table 3, and K-fold cross-validation results, as shown in Table 4, are examined on an algorithm basis, it can be said that the parameter optimization process positively affects the prediction performance of the algorithms in general. When the algorithms are evaluated individually, it can be said that the success of the Elastic net, SVR, XGB, and K-NN algorithms has increased significantly with the optimization process. When Table 4 is examined, it can be observed that there is no over-fitting situation among the algorithms. Model hyperparameters were adjusted using a grid search method in conjunction with 5-fold cross-validation to improve predictive performance. A predetermined search space was created for each algorithm using preliminary exploratory runs and suggested parameter ranges from the literature. Performance consistency was achieved by using *RMSE*, *MAE*, and R^2 scores to determine the

optimal hyperparameters of the algorithms. In the 5-fold cross-validation process, all folds were run, and the dataset was fully analyzed. The optimal values for algorithm parameters were determined in these folds. Due to the large number of parameters in the LSTM algorithm, the grid search application process took longer, but this was overcome through Bayesian optimization. The parameter values obtained after the optimization are presented in Table 5. Figure 22 depicts algorithm performances before and after the optimization process.

Table 5 Hyperparameters of algorithms

Algorithm	Hyperparameter
Elastic net	*'alpha': 0.01, 'l1_ratio': 0.99*
SVR	*'kernel': ['rbf'], 'C': [100], 'epsilon': [0.1]*
Lasso	*'alpha': 0.1*
Ridge	*'alpha': 1*
R. forest	*'max_depth': None, 'max_features': 'auto', 'min_samples_leaf': 1, 'min_samples_split': 2, 'n_estimators': 500*
XGB	*'colsample_bytree': 1.0, 'learning_rate': 0.1, 'max_depth': 10, 'n_estimators': 500, 'subsample': 0.9*
K-NN	*'n_neighbors': 3, 'p': 1, 'weights': 'distance'*
Multiple-l. r.	*'alpha': 1*
LSTM	*'units': 64, 'activation': 'tanh', 'dropout': 0.2, 'optimizer': 'adam', 'learning_rate': 0.001, 'batch_size': 32, 'epochs': 100*

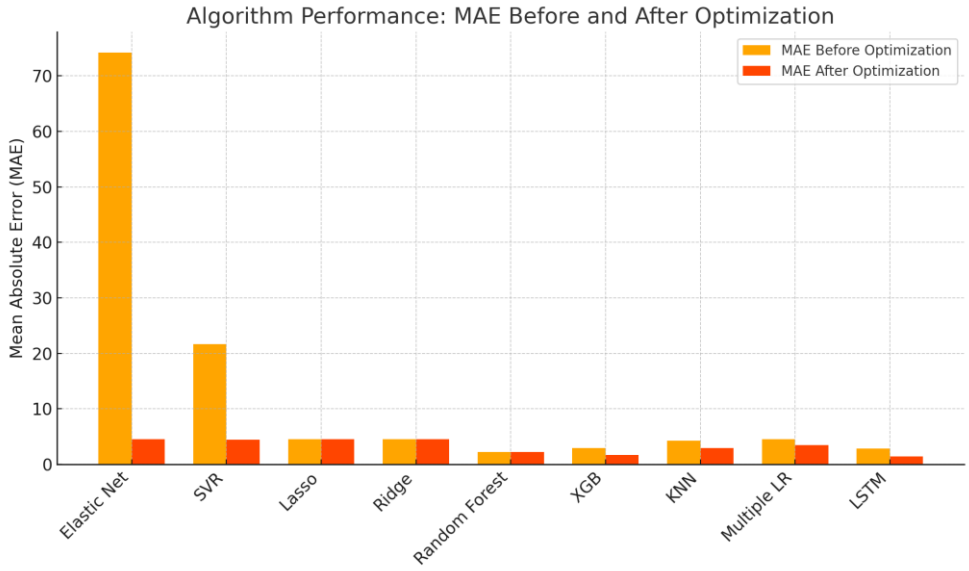

Fig. 22 Comparison of algorithm performances before and after parameter optimization process

5. Conclusions and recommendations

In hybrid ships, battery systems have an essential function in decreasing fuel consumption and increasing energy efficiency. By employing energy from batteries, the vessel may decrease its fuel consumption and move closer to its carbon reduction targets. Therefore, this study aims to estimate the RUL of the battery system in hybrid commercial vessels. By developing an approach to accurately predict the RUL, the study works toward enhancing the efficient utilization of the battery system and optimizing its performance. Simulation studies show that the RUL of the battery system on ships can be estimated with a high degree of accuracy via data-driven approaches. This level of precision provides operators with confidence in the information about various maintenance and handling activities and ensures the ship's power plant is made more robust against electrical faults in case of a possible battery system problem. Additionally, the

findings of this work will ensure timely interventions and prolong the operational lifetime of the batteries aboard the vessel.

As a result of the study, the RUL of the battery in hybrid ships has been successfully estimated by data-driven algorithms. The following information can be accessed in light of the study results: To increase operational and maintenance sustainability in hybrid ships, estimating the RUL of the battery with high success is essential in predictive maintenance-attention studies. The case study analysis revealed that the LSTM algorithm shows sufficient success in the estimation process when the parameter optimization was performed in the first stage. However, after the optimization process, its success increased. It became the most successful algorithm among the algorithms explicitly considered for the problem of estimating the RUL in hybrid ships. The case study analysis shows that the success of the XGB, Elastic Net, SVR, and K-NN algorithms also increased significantly after the optimization process. It can also be concluded from the simulation results that the performance of the Lasso, Ridge, Random forest, and Multiple-linear regression algorithms did not increase as much as the other algorithms considered after the optimization process. The practical value of the RUL estimation strategy proposed in the study lies in its predictive performance, as well as its suitability for integration into the hybrid ship Energy Management System (EMS). A high predicted RUL value will allow the EMS to better adjust the discharge depth to reduce onboard fuel consumption. If RUL is low or approaches critical thresholds, the opposite will occur. High C-rates can be limited, shifting the drive load to generators and increasing fuel consumption. Furthermore, scenarios where temperature is limited can be implemented to slow down deterioration. All these factors demonstrate that RUL estimation and management is not a standalone task but a methodology that can incorporate situational and analytical strategies. The ability of LSTM to capture nonlinear temporal dynamics associated with knee-point degradation, which rule-based and tree-based models frequently fail to adequately represent, is responsible for its superior performance, especially in the late-life region. It is naturally expected that the LSTM algorithm discussed in this study will outperform other algorithms thanks to its ability to capture temporal dependencies in battery degradation. However, when linear regression and tree-based models are treated as independent observations, it can be predicted that their predictive accuracy will be limited. The fact that each charge-discharge cycle affects the battery's aging status has limited the predictive power of such algorithms. However, the LSTM algorithm's performance in preserving the degradation model and modeling nonlinear behavior has also affected the prediction results. These features of LSTM make it stand out among other algorithms for modeling situations such as the irregular load regimes encountered in hybrid ship operations, the varying temperatures encountered onboard ships, and frequent peak power demands. It should be noted that a single hybrid electric vessel is the source of the dataset for this work. As a result, intra-vessel generalization rather than cross-fleet applicability is the main focus of the current evaluation. Multi-vessel or multi-route datasets will be used in future research to confirm that the suggested model can be applied in a variety of operational and environmental scenarios. Based on the findings, it can be observed that the RUL estimation strategy provides practical value for hybrid ship operations. If the predicted RUL value can be integrated into the onboard EMS, it will enable the dynamic behavior of the onboard load-sharing strategy, reduce fuel consumption, and develop various battery protection strategies. Achieving these will increase operational efficiency and sustainability onboard.

In addition, the study acknowledges several limitations and suggestions for future research. One significant challenge is the limited availability of datasets from hybrid vessels, as the technology is still relatively new and not yet extensive. However, with increased investments in hybrid vessels and the growing adoption of such ships in the coming years, gaining access to data from these vessels will become more viable. Furthermore, as the quality and size of the data sets increase, more accurate and robust results can be achieved, leading to better analytical models and maintenance strategies. While the study's results are quite promising, they are limited by the size and scope of the dataset due to the difficulty of obtaining data from hybrid vessels and the fact that this process is not expected to accelerate significantly in the near future. With the use of much larger and more comprehensive datasets in future studies, digital twin processes will take their place in literature as a much more promising approach for determining the RUL of ships' batteries. Despite the study's important findings, it should be noted that it also has limitations. The process of obtaining data from commercial vessels is challenging, and because the data was collected from a single hybrid ship, the results

cannot be generalized. Furthermore, the data was collected as historical data rather than real-time monitoring. Future studies can obtain much more robust data by diversifying and strengthening IoT and sensor systems.

ACKNOWLEDGMENTS

This study was supported by Istanbul Technical University Scientific Research Projects Coordination Office with project code MDA-2024-45607.

REFERENCES

[1] Perčić, M., Frković, L., Pukšec, T., Ćosić, B., Li, O.L., Vladimir, N., 2022. Life-Cycle Assessment and Life-Cycle Cost Assessment of Power Batteries for All-Electric Vessels for Short-Sea Navigation. *Energy*, 251, 123895. https://doi.org/10.1016/j.energy.2022.123895

[2] Lazakis, I., Raptodimos, Y., Varelas, T., 2018. Predicting Ship Machinery System Condition through Analytical Reliability Tools and Artificial Neural Networks. *Ocean Engineering*, 152, 404-415. https://doi.org/10.1016/j.oceaneng.2017.11.017

[3] Bataille, C., Åhman, M., Neuhoff, K., Nilsson, L.J., Fischedick, M., Lechtenböhmer, S., et al., 2018. A Review of Technology and Policy Deep Decarbonization Pathway Options for Energy-Intensive Industry Production Consistent with the Paris Agreement. *Journal of Cleaner Production*, 187, 960-973. https://doi.org/10.1016/j.jclepro.2018.03.107

[4] Sui, C., de Vos, P., Stapersma, D., Visser, K., Ding, Y., 2020. Fuel Consumption and Emissions of Ocean-Going Cargo Ship with Hybrid Propulsion and Different Fuels over Voyage. *Journal of Marine Science and Engineering*, 8(8), 588. https://doi.org/10.3390/jmse8080588

[5] Dinh, T.Q., Bui, T.M.N., Marco, J., Watts, C., Yoon, J.I., 2018. Optimal Energy Management for Hybrid Electric Dynamic Positioning Vessels. *IFAC-PapersOnLine*, 51(29), 98-103. https://doi.org/10.1016/j.ifacol.2018.09.476

[6] Wu, B., Li, C., Hu, J., Wang, L., Li, Y., 2020. Reinforcement Learning-Based Energy Management for Hybrid Electric Passenger Ship. *Energy*, 198, 117288. https://doi.org/10.1016/j.energy.2020.117288

[7] Nuchturee, C., Li, T., Xia, H., 2020. Energy Efficiency of Integrated Electric Propulsion for Ships – A Review. *Renewable and Sustainable Energy Reviews*, 134, 110145. https://doi.org/10.1016/j.rser.2020.110145

[8] Ghenai, C., Bettayeb, M., Brdjanin, B., Hamid, A.K., 2019. Hybrid Solar PV/PEM Fuel Cell/Diesel Generator Power System for Cruise Ship: A Case Study in Stockholm, Sweden. *Case Studies in Thermal Engineering*, 14, 100497. https://doi.org/10.1016/j.csite.2019.100497

[9] Kolodziejski, M., Michalska-Pozoga, I., 2023. Battery Energy Storage Systems in Ships' Hybrid/Electric Propulsion Systems. *Energies*, 16(3), 1122. https://doi.org/10.3390/en16031122

[10] Hoang, A. T., Bui, T. A. E., Nguyen, X. P., Bui, V. H., Nguyen, Q. C., Truong, T. H., Chung, N., 2025. Explainable Machine Learning-Based Prediction of Fuel Consumption in Ship Main Engines Using Operational Data. *Brodogradnja*, 76(4), 76405. https://doi.org/10.21278/brod76405

[11] Jianyun, Z., Li, C., Lijuan, X., Bin, W., 2019. Bi-Objective Optimal Design of Plug-In Hybrid Electric Propulsion System for Ships. *Energy*, 177, 247-261. https://doi.org/10.1016/j.energy.2019.04.079

[12] Meng, L., Gan, H., Liu, H., Lu, D., 2025. Deep Learning-Based Research on Fault Warning for Marine Dual Fuel Engines. *Brodogradnja*, 76(3), 76303. https://doi.org/10.21278/brod76303

[13] Geertsma, R.D., Negenborn, R.R., Visser, K., Hopman, J.J., 2017. Design and Control of Hybrid Power and Propulsion Systems for Smart Ships: A Review of Developments. *Applied Energy*, 194, 30-54. https://doi.org/10.1016/j.apenergy.2017.02.060

[14] Ritari, A., Huotari, J., Halme, J., Tammi, K., 2020. Hybrid Electric Topology for Short-Sea Ships with High Auxiliary Power Availability Requirement. *Energy*, 190, 116359. https://doi.org/10.1016/j.energy.2019.116359

[15] Lindstad, H.E., Eskeland, G.S., Rialland, A., 2017. Batteries in Offshore Support Vessels – Pollution, Climate Impact and Economics. *Transportation Research Part D: Transport and Environment*, 50, 409-417. https://doi.org/10.1016/j.trd.2016.11.023

[16] Tahir, M.U., Anees, M., Khan, H.A., Khan, I., Zaffar, N., Moaz, T., 2021. Modeling and Evaluation of Nickel Manganese Cobalt-Based Li-Ion Storage for Stationary Applications. *Journal of Energy Storage*, 36, 102346. https://doi.org/10.1016/j.est.2021.102346

[17] Tahir, M.U., Sangwongwanich, A., Stroe, D.I., Blaabjerg, F., 2023. Overview of Multi-Stage Charging Strategies for Li-Ion Batteries. *Journal of Energy Chemistry*, 84, 228-241. https://doi.org/10.1016/j.jechem.2023.05.023

[18] Adam, A., Wandt, J., Knobbe, E., Bauer, G., Kwade, A., 2020. Fast-Charging of Automotive Lithium-Ion Cells: In-Situ Lithium-Plating Detection and Comparison of Different Cell Designs. *Journal of The Electrochemical Society*, 167(13), 130503. https://doi.org/10.1149/1945-7111/abb564

[19] Lee, J., Sun, H., Liu, Y., Li, X., 2024. A Machine Learning Framework for Remaining Useful Lifetime Prediction of Li-Ion Batteries Using Diverse Neural Networks. *Energy and AI*, 15, 100319. https://doi.org/10.1016/j.egyai.2023.100319

[20] Chen, J., Li, P., Wu, L., 2025. Joint prediction of SOH and RUL of lithium-ion batteries using single-cycle charging data. *Energy*, 336, 138351. https://doi.org/10.1016/j.energy.2025.138351

[21] Su, S., Miao, Z., Zhao, Y., Song, N., 2024. Digitally Twin Driven Ship Cooling Pump Fault Monitoring System and Application Case. *Brodogradnja*, 75(4), 75403. https://doi.org/10.21278/brod75403

[22] Liu, Z., Chu, Y., Li, G., Hildre, H.P., Zhang, H., 2024. Shipboard Crane Digital Twin: An Empirical Study on R/V Gunnerus. *Ocean Engineering*, 302, 117675. https://doi.org/10.1016/j.oceaneng.2024.117675

[23] Xia, Y., Zhang, Y., Li, C., Wang, S., 2021. A Deep Learning Approach for Predicting the Remaining Useful Life of Lithium-Ion Batteries. *Applied Energy*, 283, 116263. https://doi.org/10.1016/j.apenergy.2020.116263

[24] Patonai, Z., Kicsiny, R., Géczi, G., 2022. Multiple Linear Regression-Based Model for the Indoor Temperature of Mobile Containers. *Heliyon*, 8, e12098. https://doi.org/10.1016/j.heliyon.2022.e12098

[25] Luu, Q.H., Lau, M.F., Ng, S.P.H., Chen, T.Y., 2021. Testing Multiple Linear Regression Systems with Metamorphic Testing. *Journal of Systems and Software*, 182, 111062. https://doi.org/10.1016/j.jss.2021.111062

[26] Li, D., Gu, M., Liu, S., Sun, X., Gong, L., Qian, K., 2022. Continual Learning Classification Method with the Weighted k-Nearest Neighbor Rule for Time-Varying Data Space Based on the Artificial Immune System. *Knowledge-Based Systems*, 240, 108145. https://doi.org/10.1016/j.knosys.2022.108145

[27] Gkerekos, C., Lazakis, I., Theotokatos, G., 2019. Machine Learning Models for Predicting Ship Main Engine Fuel Oil Consumption: A Comparative Study. *Ocean Engineering*, 188, 106282. https://doi.org/10.1016/j.oceaneng.2019.106282

[28] Nguyen, H.D., Truong, G.T., Shin, M., 2021. Development of Extreme Gradient Boosting Model for Prediction of Punching Shear Resistance of R/C Interior Slabs. *Engineering Structures*, 235, 112067. https://doi.org/10.1016/j.engstruct.2021.112067

[29] Wang, X.G., Zou, Z.J., Hou, X.R., Xu, F., 2015. System identification modelling of ship manoeuvring motion based on ε - Support vector regression. *Journal of Hydrodynamics*, 27, 502-512. https://doi.org/10.1016/S1001-6058(15)60510-8

[30] Haq, E.U., Huang, J., Xu, H., Li, K., Ahmad, F., 2021. A Hybrid Approach Based on Deep Learning and Support Vector Machine for the Detection of Electricity Theft in Power Grids. *Energy Reports*, 7, 349-356. https://doi.org/10.1016/j.egyr.2021.08.038

[31] Zheng, Y., Ge, Y., Muhsen, S., Wang, S., Elkamchouchi, D.H., Ali, E., Ali, H.E., 2023. Advances in Engineering Software New ridge regression , artificial neural networks and support vector machine for wind speed prediction. *Advances in Engineering Software*, 179, 103426. https://doi.org/10.1016/j.advengsoft.2023.103426

[32] Giri, S., Kang, Y., MacDonald, K., Tippett, M., Qiu, Z., Lathrop, R.G., Obropta, C.C., 2023. Revealing the Sources of Arsenic in Private Well Water Using Random Forest Classification and Regression. *Science of The Total Environment*, 857, 159360. https://doi.org/10.1016/j.scitotenv.2022.159360

[33] Laurie, A., Anderlini, E., Dietz, J., Thomas, G., 2021. Machine Learning for Shaft Power Prediction and Analysis of Fouling-Related Performance Deterioration. *Ocean Engineering*, 234, 108886. https://doi.org/10.1016/j.oceaneng.2021.108886

[34] Zhou, T., Hu, Q., Hu, Z., Zhen, R., 2022. An adaptive hyper parameter tuning model for ship fuel consumption prediction under complex maritime environments. *Journal of Ocean Engineering and Science*, 7, 255-263. https://doi.org/10.1016/J.JOES.2021.08.007

[35] Assaf, A.G., Tsionas, M., Tasiopoulos, A., 2019. Diagnosing and Correcting the Effects of Multicollinearity: Bayesian Implications of Ridge Regression. *Tourism Management*, 71, 1-8. https://doi.org/10.1016/j.tourman.2018.09.008

[36] Moreno-Salinas, D., Moreno, R., Pereira, A., Aranda, J., de la Cruz, J.M., 2019. Modelling of a Surface Marine Vehicle with Kernel Ridge Regression Confidence Machine. *Applied Soft Computing*, 76, 237-250. https://doi.org/10.1016/j.asoc.2018.12.002

[37] Wong, T.T., 2017. Parametric methods for comparing the performance of two classification algorithms evaluated by k-fold cross validation on multiple data sets. *Pattern Recognition*. 65, 97-107. https://doi.org/10.1016/j.patcog.2016.12.018

[38] Liu, Z., Gao, J., Xu, L., Jia, P., Pan, D., Xue, W., 2022. Electromagnetic Fusion Underwater Positioning Technology Based on ElasticNet Regression Method. Proc. *IEEE 10th International Conference on Information, Communication and Networks* (ICICN), August 23-24, Zhanye, China, 121-126. https://doi.org/10.1109/ICICN56848.2022.10006453

[39] Wang, S., Ji, B., Zhao, J., Zhao, J., Zhao, D., 2022. Remaining Useful Life Prediction for Lithium-Ion Battery Using a Hybrid Model Based on Improved LSTM and Particle Filter. *Energy*, 238, 121724. https://doi.org/10.1016/j.energy.2021.121724

[40] Joseph, R.V., Mohanty, A., Tyagi, S., Mishra, S., Satapathy, S.K., Mohanty, S.N., 2022. A Hybrid Deep Learning Framework with CNN and Bi-Directional LSTM for Store Item Demand Forecasting. *Computers and Electrical Engineering*, 103, 108358. https://doi.org/10.1016/j.compeleceng.2022.108358

[41] Ling B, Yu L, Zhang Y, Tang J, Zhou Y, Ji K, Guo R., 2025.Cross-validation assisted hybrid dataset construction for low-cost and accurate prediction of photovoltaic global maximal power point under partial shading conditions. *Energy Reports*, 14, 2732-2754. https://doi.org/10.1016/j.egyr.2025.09.036

[42] Saud, S., Jamil, B., Upadhyay, Y., Irshad, K., 2020. Performance Improvement of Empirical Models for Estimation of Global Solar Radiation in India: A K-Fold Cross-Validation Approach. *Sustainable Energy Technologies and Assessments*, 40, 100768. https://doi.org/10.1016/j.seta.2020.100768

[43] Ling, H., Qian, C., Kang, W., Liang, C., Chen, H., 2019. Combination of Support Vector Machine and K-Fold Cross Validation to Predict Compressive Strength of Concrete in Marine Environment. *Construction and Building Materials*, 206, 355-363. https://doi.org/10.1016/j.conbuildmat.2019.02.071

[44] Olson, L.M., Qi, M., Zhang, X., Zhao, X., 2021. Machine Learning Loss Given Default for Corporate Debt. *Journal of Empirical Finance*, 64, 144-159. https://doi.org/10.1016/j.jempfin.2021.08.009

[45] Frías-Paredes, L., Mallor, F., Gastón-Romeo, M., León, T., 2018. Dynamic Mean Absolute Error as a New Measure for Assessing Forecasting Errors. *Energy Conversion and Management*, 162, 176-188. https://doi.org/10.1016/j.enconman.2018.02.030

[46] Wun, L.M., Pearn, W.L., 1991. Assessing the statistical characteristics of the mean absolute error or forecasting. *International Journal of Forecasting*, 7, 335-337. https://doi.org/10.1016/0169-2070(91)90007-I

[47] Ćalasan, M., Abdel Aleem, S.H.E., Zobaa, A.F., 2020. On the Root Mean Square Error (RMSE) Calculation for Parameter Estimation of Photovoltaic Models: A Novel Exact Analytical Solution Based on Lambert W Function. *Energy Conversion and Management*, 210, 112716. https://doi.org/10.1016/j.enconman.2020.112716

[48] Karunasingha, D.S.K., 2022. Root Mean Square Error or Mean Absolute Error? Use Their Ratio as Well. *Information Sciences*, 585, 609-629. https://doi.org/10.1016/j.ins.2021.11.036

[49] Cheng, C.L., Shalabh, Garg, G., 2014. Coefficient of Determination for Multiple Measurement Error Models. *Journal of Multivariate Analysis*, 126, 137-152. https://doi.org/10.1016/j.jmva.2014.01.006

[50] Ueki, M., 2021. Testing Conditional Mean Through Regression Model Sequence Using Yanai's Generalized Coefficient of Determination. *Computational Statistics & Data Analysis*, 158, 107168. https://doi.org/10.1016/j.csda.2021.107168

[51] Barillaro L. Deep learning platforms: TensorFlow. 2025. *Encyclopedia of Bioinformatics and Computational Biology (2nd ed.)*. Amsterdam: Elsevier. 171-174. https://doi.org/10.1016/B978-0-323-95502-7.00167-6